Available online at www.sciencedirect.com
ScienceDirect
Ceramics International 35 (2009) 2577–2585
CERAMICS INTERNATIONAL
www.elsevier.com/locate/ceramint

Processing of micro-components made of sintered reaction-bonded silicon nitride (SRBSN). Part 1: Factors influencing the reaction-bonding process

Marcus Müller *, Werner Bauer, Regina Knitter

Forschungszentrum Karlsruhe, Institute for Materials Research III, PO-Box 3640, D-76021 Karlsruhe, Germany

Received 4 December 2008; received in revised form 22 January 2009; accepted 14 February 2009
Available online 11 March 2009

Abstract

In order to establish a process for the manufacturing of injection moulded micro-components of sintered reaction-bonded silicon nitride (SRBSN) several process parameters were investigated with regard to their influence on the reaction-bonding step. One question to be answered was how the sintering aids affect the nitridation behaviour of a silicon green body. For the processing of micro-components it was of special interest to study, how a decreasing sample size and wall thickness would influence the rate of Si_3N_4 formation. By varying the added amounts of the sintering aids, it was found that increasing the Y_2O_3 and MgO contents both improved the nitridation rate, whereas an increase of Al_2O_3 content resulted in reduced nitridation rates. Within the investigated range of sample dimensions (0.2–4.0 g) the unexpected observation was made, that with decreasing sample weight the nitridation rate also decreased. This was explained by the exothermic nature of the reaction between Si and N_2 and the fact that small samples with a large surface-to-volume ratio attain thermal equilibrium with their environment better than large samples which may be subject to local overheating.

Keywords: A. Injection moulding; D. Si_3N_4; Reaction-bonding; Micro-components

1. Introduction

Silicon nitride (Si_3N_4) ceramics cover a wide range of advantageous properties like low weight, good mechanical and thermo-mechanical behaviour, as well as wear and corrosion resistance which make them to be valued materials especially for structural applications [1–3]. Amongst the numerous modifications of Si_3N_4 *sintered reaction-bonded silicon nitride* (SRBSN) can be considered as a favourable compromise between the high-performance sintered Si_3N_4 (SSN) and the low-cost reaction-bonded Si_3N_4 (RBSN). Analogous to the RBSN process, SRBSN silicon nitride is generated in situ by direct nitridation of Si. A following post-sintering step at higher temperatures with the presence of sintering aids diminishes the considerable porosity which still exists after reaction-bonding. By this densification, 93–99% of theoretical density can be realized and thus mechanical properties which are comparable to hot-pressed (HPSN) or conventionally sintered (SSN) silicon nitride [3–5]. But in contrast to SSN, cost-effective (metallurgical) silicon qualities can be used as raw material instead of expensive Si_3N_4 powder.

As a consequence of the volume increase during RBSN formation the ‘‘green density’’ is significantly higher than for green bodies prepared from Si_3N_4 powder. The resulting sintering shrinkage for full densification is correspondingly lower in the case of SRBSN. This aspect renders SRBSN interesting for near net-shape manufacturing where a reduced sintering shrinkage should enable narrower dimensional tolerances [6]. Especially micro-components or micro-patterned parts demand high precision from the manufacturing process as final machining is excluded for economical and practical reasons.

It was the aim of the present work to investigate to what extent SRBSN is suited for the fabrication of high-strength ceramic micro-parts. One boundary condition was the ability for medium and large scale production, and therefore injection moulding was chosen as a well established technology for the fabrication of complex-shaped parts. The application of injection moulding for the processing of SRBSN micro-parts implies also the development of appropriate feedstocks, where

* Corresponding author. Tel.: +49 7247 822310; fax: +49 7247 824612.
E-mail address: marcus.mueller@imf.fzk.de (M. Müller).

0272-8842/$36.00
doi:10.1016/j.ceramint.2009.02.013

the silicon powder and the sintering aids are compounded with a binder. Besides the necessity of adapted flow behaviour of the feedstock to replicate even very delicate patterns, it has to be considered how the microstructure and the properties of the SRBSN components are influenced by the moulding process. In the literature a lot of work is published on the processing and properties of SRBSN [1,5,7–13]. Most of these investigations, however, were carried out with powder compacts (axially or isostatically pressed) containing no or only minor binder fractions, whereas in injection moulding the binder phase reaches 40–50 vol% of the green body. Debinding of injection moulded components is a crucial step during thermal treatment as large amounts of liquid or gaseous binder fractions have to be removed without destroying the physical integrity of the part. For defect-free debinding the formation of an open pore network with sufficient pore width is obligatory. The same pore structure then allows for a subsequent homogenous nitridation of the debinded Si body.

Micro-manufacturing

Although manufacturing of (S)RBSN via injection moulding has been described before [14–17], to our knowledge it has yet not been applied for the fabrication of *micro*-parts. To adopt a processing technology to smaller dimensions some micro-specific features have to be considered [18]. An important factor when changing from the macro to the micro-world is the increase of surface-to-volume ratio with decreasing size. For macroscopic or thick-walled components the diffusion of nitrogen into the inner regions might become limiting especially when the pore cross-section becomes smaller in the course of the reaction. Also the exothermic character of silicon nitride formation, which may cause melting of the powder compact, has to be tackled [7]. Both pore diffusion and dissipation of heat become minor problems when small components with high surface area have to be formed, and consequently faster processing is possible. On the other side the higher surface-to-volume ratio is responsible for the fact that the mechanical properties of micro-parts are increasingly dominated by the defect density of the surface region [19,20]. It is, therefore, essential that the mechanical properties are determined on the basis of samples with correspondingly reduced dimensions.

To establish a stable manufacturing process – which is a prerequisite for good reproducibility and narrow tolerances – the main influencing process parameters had to be identified. Special attention was paid to the reaction-bonding step in which the intrinsic material Si_3N_4 is primarily formed. Several studies and reviews describe and discuss the reactions between silicon and nitrogen in detail [21–25] and reveal that – amongst others – the reaction rate is strongly influenced by the Si impurity level. Moreover, metals or metal oxides like Fe, Cr, Ca, Cu, Ag, and Zr are known to have a catalytic effect on Si nitridation [26,27]. As for the processing of SRBSN the sintering aids (e.g. Y_2O_3, Al_2O_3, and MgO) usually are added in substantial amounts to the Si powder, in this case an effect on the nitridation behaviour is also very likely. Most studies on SRBSN deal with the influence of sintering aids on the densification behaviour or the thermo-physical and mechanical properties of the *sintered* material [5,8–11]. Only few studies, e.g. Lee and Kim [28] and Zhang [29] focussed on the interaction of sintering aids and nitridation behaviour of reaction-bonded silicon nitride. Their approach is picked up now and extended to varying concentrations and combinations of the common sintering aids Y_2O_3, Al_2O_3, and MgO.

The present paper, which is intended as the first of two parts, is confined to the reaction-bonding step (without post-sintering) and how the metal oxide additions – introduced primarily to facilitate liquid phase sintering at temperatures of 1700 °C and higher – already effect the silicon nitride formation at temperatures below 1400 °C. In view of the aimed application as structural material for micro-components also the question arises, if a smaller sample size will allow a faster nitridation process.

2. Experimental

For the sample preparation a modified low-pressure injection moulding (LPIM) technique was applied. When only prototypes or small number of identical samples are required, the flexible LPIM technique offers several advantages as a fast and cost effective manufacturing that is characterized by markedly low equipment and tooling costs [30]. A subsequent transfer of the experimental findings to conventional (high-pressure) powder injection moulding (HPIM) with its medium or large series production capability is eased as both processes are closely related.

2.1. Powder and feedstock preparation

As starting material Si powder (SiMP grade AX05, HC Starck, Germany) with a mean diameter d_{50} of 3.9 μm was used. To reduce the particle size and for homogeneous distribution of the sintering aids, Si powder was planetary ball milled together with varying amounts of Y_2O_3 (Aldrich, 99.99%, d_{50} = 3.4 μm), Al_2O_3 (Ceralox SPA05, d_{50} = 0.35 μm) and MgO (Merck, p.a. d_{50} = 0.25 μm) for 20–48 h in 2-propanol using zirconia beaker and balls. After ball milling the powder blends were dried, sieved, and characterized according to their average particle size (Dispersion Technology, DT1200) and BET specific surface area (Flow Sorb II, Micromeritics), as shown in Table 1.

Low-pressure injection moulding requires low-viscosity feedstocks and therefore a paraffin wax (Terhel 6403, Schüman Sasol) was used as main binder component. Furthermore, dispersants were added to ease wetting of the powder blend by the nonpolar binder, to stabilize the feedstock against segregation, and to control the rheological behaviour of the feedstock. The following dispersants were added to the molten paraffin: ODTMS (octadecyltetramethoxysilane, 90% in ethanol, Aldrich), Hypermer LP1 (Uniquema), and a N-alkylsuccinimide (OLOA 1200, Chevron). The feedstocks were prepared by adding the powder blends to the molten paraffin/dispersant mixture at a temperature of 95 °C. For homogeniza-

Table 1
Powder and feedstock characteristics and resulting Si conversion.

Feedstock	Sintering aid percentage			BET (m^2/g)	d_{50} (μm)	S.L.[a] (vol%)	Rel. nitridation[b] (%)
	Y_2O_3 (wt.%)	Al_2O_3 (wt.%)	MgO (wt.%)				
YA-1	8.0	3.2	–	6.8	1.3	56.5	53.2 ± 1.2
YA-2	8.0	3.2	–	8.8	1.0	61.0	50.6 ± 1.4
YA-3	12.3	3.0	–	6.3	1.8	56.4	78.8 ± 1.2
YA-4	12.3	3.0	–	9.1	1.2	56.2	76.1 ± 4.1
YA-5	12.3	1.7	–	7.8	1.2	56.6	90.4 ± 3.2
YM-1	12.4	–	0.7	10.5	0.7	57.1	81.1 ± 3.9
YM-2	12.3	–	3.0	7.1	1.7	55.6	92.9 ± 0.2
YM-3	12.3	–	3.0	7.1	1.7	60.0	93.7 ± 0.9
YAM-1	12.3	1.5	1.5	6.3	1.3	56.8	92.9 ± 0.2
YAM-2	12.3	1.5	1.5	10.1	1.0	56.9	91.8 ± 0.2

[a] Feedstock solid loading.
[b] After 1390 °C, 4 h.

tion a dissolver stirrer (VMA Getzman Verfahrenstechnik, Reichshof, Germany) was used which allowed to prepare the feedstocks at vacuum conditions. Feedstock solid loadings were set to 56–61 vol%, and the corresponding shear viscosity was measured using a MCR 300 rheometer (Paar Physica, Stuttgart, Germany). For the measurements with shear stress control (1–3000 Pa) and plate/plate geometry the temperature was kept constant at 85 °C. The viscosity at a shear rate of 100 s^{-1} was picked out as representative value.

2.2. Moulding

One of the main advantages of LPIM is the possibility to use soft moulds due to the moderate injection pressure of only 0–3 bar. Even silicone rubber moulds will work and their preparation is simple, fast, and inexpensive as they are obtained within hours just by copying a master model made of any material. Due to the low feedstock viscosities in the order of 10 Pa s complete mould filling was achieved just by casting the feedstock into preheated silicone moulds at 90–100 °C. Entrapped air was evacuated afterwards from the filled mould while the feedstock was still liquid. High mould elasticity and low adhesion forces facilitate the demoulding even of complex-shaped parts after cooling down to room temperature. Fig. 1 illustrates the sample geometries used for the determination of the sample size influence on the nitridation behaviour. The column array serves primarily as a supply for a large number of identically prepared specimens for micro-bending tests.

2.3. Thermal treatment

The paraffin binder was burned-out in air atmosphere using a furnace with air circulation and exhausting the volatile pyrolysis products (Carbolite HT6/28), absorptive supports like porous ceramic plates or powder beds were applied to promote the removal of liquid binder phase. The maximum temperature during debinding was limited to 500 °C where about 95% of the binder is withdrawn and significant oxidation of the Si powder is still avoided. The small amount of residual carbon is beneficial as it preserves a sufficient mechanical stability for handling the samples.

The reaction-bonding step was performed in a furnace equipped with tungsten heating elements, with the debinded samples placed in BN crucibles. The standard program comprised a heating rate of 10 K/min up to 1390 °C, a cooling rate of 20 K/min, and a dwell time of 4 h. A static atmosphere with 95% nitrogen and 5% hydrogen (forming gas) at an overall pressure of 0.16 MPa was applied. Due to the Si_3N_4 formation the pressure decreased continuously during dwell time, when it dropped below 0.15 MPa new forming gas was added until 0.16 MPa was reached again.

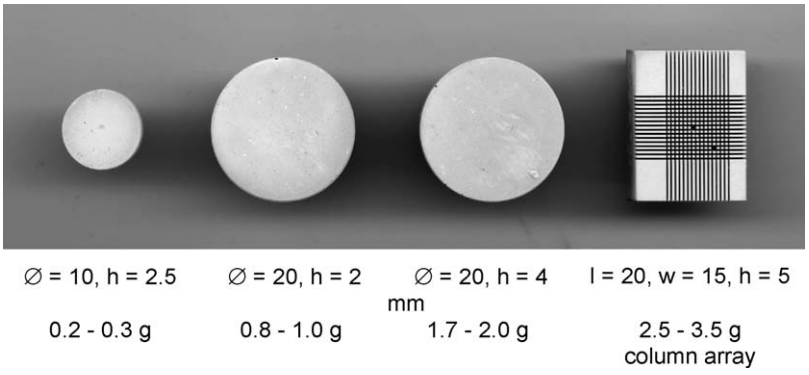

Fig. 1. Dimensions and weight of different sample geometries for the nitridation investigations, shown in the RBSN state, i.e. after nitridation.

The amount of Si conversion in the reaction-bonded samples was calculated by determining the weight increase the debinded samples gained during nitridation and by correlating the weight increase with the theoretical value of 66.5% (1 − (mol. weight Si_3N_4/(3 × mol. weight Si))) and the fraction of Si in the starting powder blend. After nitridation qualitative phase analysis was conducted on polished cross-sections by X-ray diffraction (XRD) in step scan mode using Cu Kα radiation (Siemens D5005).

3. Results

3.1. Effect of sintering aids

Table 1 comprises the investigated variations of sintering aids and the particle properties of the powder blends after planetary ball milling (BET specific surface area and d_{50} value). Most methods for particle size measurement reach their limits when fine powder mixtures of materials with different physical properties (transparency and density) have to be characterized. The d_{50} value therefore must not be over-interpreted, but as all powder blends predominantly consist of silicon a relative assessment should be approvable.

Furthermore the solid loading of the different feedstocks is presented in Table 1, together with the degree of Si conversion into Si_3N_4 (relative nitridation) which refers to samples of the column array type. The nitridation results were obtained using the following process parameters: temperature of 1390 °C, dwell time of 4 h and forming gas atmosphere (95% N_2 and 5% H_2).

Commonly used concentrations of sintering aids for liquid phase sintering of Si_3N_4 are 5 wt.% yttria and 2 wt.% alumina. Taking into account the weight gain during Si_3N_4 formation, Si has to be doped correspondingly with 8 wt.% yttria and 3.2 wt.% alumina. With this composition two blends were prepared (YA-1 and YA-2) revealing slightly different average grain sizes, which were obtained by extending planetary ball milling time (21 h for YA-1 and 40 h for YA-2). After 4 h at 1390 °C approximately 50% of Si reacted to Si_3N_4; thereby the samples with the finer powder (YA-2) exhibited slightly lower yields (51% instead of 53%). The Si conversion was increased significantly to 76–79% by increasing the Y_2O_3 fraction to 12.3% while keeping the Al_2O_3 addition constant (YA-3 and YA-4). Again the finer powder corresponds to the somewhat lower conversion. Even higher Si_3N_4 yields of about 90% were achieved by reducing the Al_2O_3 content from 3.0% to 1.7% (YA-5).

Another set of powder blends with MgO instead of Al_2O_3 were prepared with varying MgO additions at constant Y_2O_3 content (YM1-3), presenting an increase of Si conversion with increasing MgO content (>93% with 3 wt.% MgO). For the preparation of feedstocks YM-2 and YM-3 the same ball milled powder blends were applied, but different dispersants – i.e. octyltetramethoxysilane for YM-2 and N-alkylsuccinimide for YM-3 – allowed for different solid loadings of 55.6% and 60%, respectively. The highest conversion of nearly 94% was found for YM-3.

The powder blends used for feedstock YAM-1and YAM-2 included both Al_2O_3 and MgO in equal fractions of 1.5 wt.%. Again an altered average grain size was generated by variation of milling time. Both feedstocks revealed high Si conversion of more than 90%, however once more the coarser powder (YAM-1) exhibited a slightly better nitridation of 93% after 4 h at 1390 °C.

Phase composition

Analysis of the X-ray diffraction spectra showed that the reaction-bonded silicon nitride samples mainly consisted of the α-phase with β-phase as minor constituent. The presence of β-Si_3N_4 indicates that a liquid phase has been formed during nitridation, enabling the α-to-β transformation. In principle a liquid phase may derive from molten Si as well as from the combination of sintering aids with the native SiO_2 layer of the Si grains. The eutectic temperatures in the Y_2O_3–Al_2O_3–SiO_2 and Y_2O_3–MgO–SiO_2 systems are reported to be at 1371 °C [31] and 1380 °C [32], respectively. Due to the presence of impurities and nitrogen in the present system, the eutectic temperatures can be expected to be even lower and hence clearly below the nitridation temperature of 1390 °C.

In Fig. 2(a)–(c) XRD pattern obtained from polished cross-sections after 4 h at 1390 °C nitridation are shown, each representing the influence of a different combination of sintering aids. For the YA-3 sample even after 4 h less than 80% of Si reacted with nitrogen and consequently a strong Si peak is visible in Fig. 2(a). Owing to higher nitridation rates the MgO containing samples from YM-3 and YAM-1 do not display any detectable signs of free Si in their diffraction patterns shown in Fig. 2(b) and (c).

In good agreement with the investigations of Lee and Kim [28] the α/β phase ratio is apparently influenced by the sintering aids in a manner that the combination of Y_2O_3 and Al_2O_3 results in slightly higher fractions of β-Si_3N_4. No significant differences can be observed in the spectra of YM-3 and YAM-1.

Beside the two silicon nitride morphologies additional crystalline secondary phases from the system Y_2O_3–SiO_2–Si_3N_4 have been detected; explicitly $Y_5Si_3O_{12}N$ (YN-apatite, $10Y_2O_3{\cdot}9SiO_2{\cdot}1Si_3N_4$) could be identified from the XRD pattern of YAM-1, and $YSiO_2N$ (YN-wollastonite, $2Y_2O_3{\cdot}1SiO_2{\cdot}1Si_3N_4$) in the spectra of YA-3 and YM-3. The relatively small MgO and Al_2O_3 additions, not exceeding 3 wt.%, were still noticeable in XRD spectra of green and debinded bodies, but could not be detected after nitridation anymore. It is concluded, that at least the main fraction of these oxides has been transformed into the glass phase.

3.2. Effect of dwell time

For column array specimens of feedstocks YA-3, YM-2, YM-3, and YAM-1 the Si conversion was determined in the dependence of dwell time in the range of 0.5–8 h. Individual samples were taken for each dwell time as repeated cooling and heating cycles with one and the same sample may cause crack formation due to thermal mismatch between Si_3N_4 and Si and

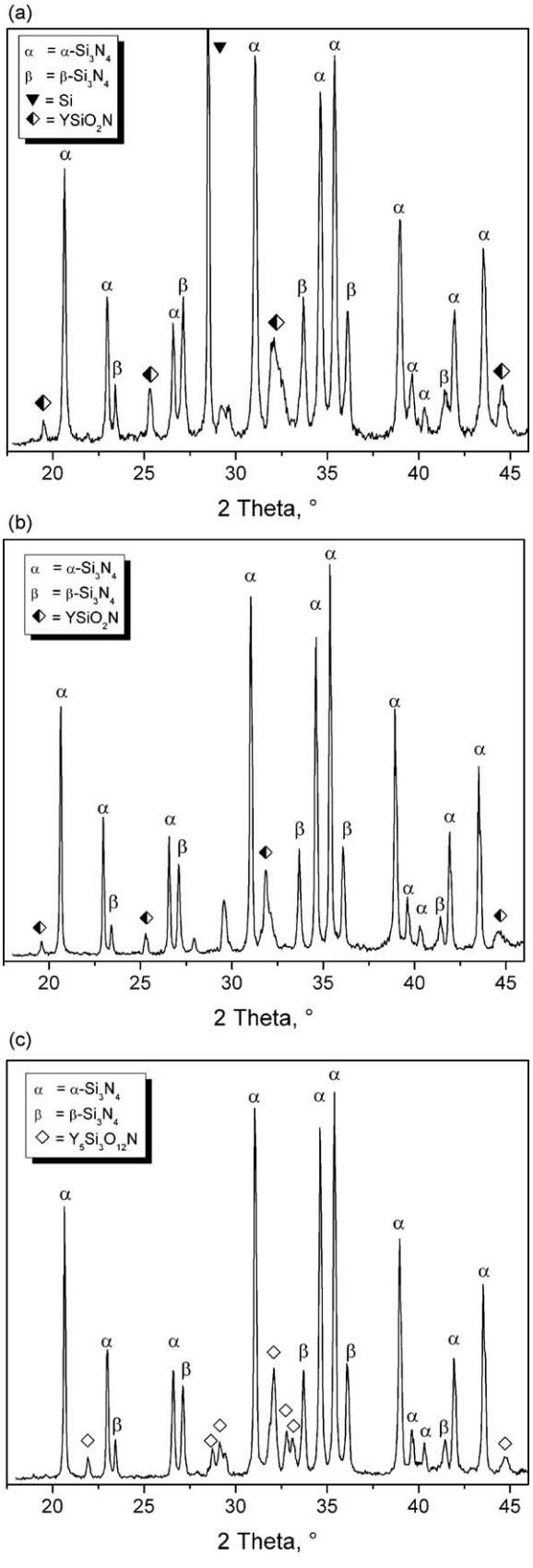

Fig. 2. XRD-spectra of polished cross-sections after nitridation at 1390 °C, 4 h: (a) YA-3, (b) YM-3, and (c) YAM-1.

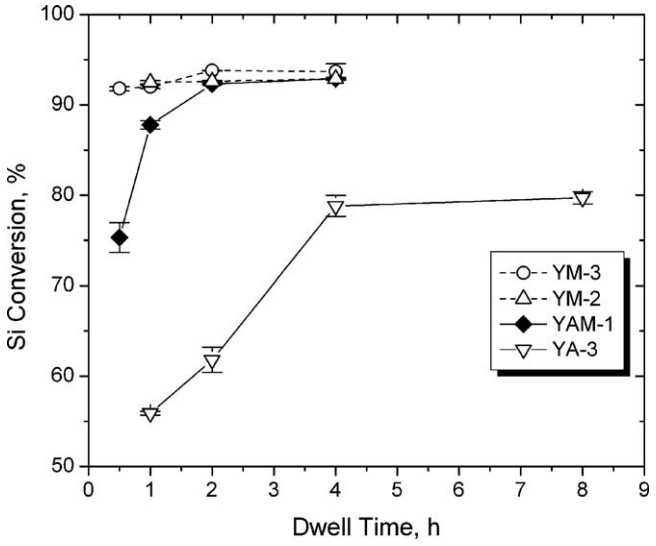

Fig. 3. Si conversion in dependence of dwell time; 1390 °C, sample geometry: column array.

would adulterate the comparison of reaction rates by creating new surfaces [33]. In Fig. 3 the Si conversion is presented revealing different nitridation rates for alumina and magnesia doped Si powder blends. For YM-2 and YM-3 already after 1 and 0.5 h, respectively, more than 90% conversion to Si_3N_4 occurred. A further increase of dwell time led to only marginal improvement. YA-3 samples revealed an approximately linear increase of conversion up to 4 h reaching a relatively low level of about 80%. By doubling the dwell time to 8 h no significant further increase is observed. Replacement of 1.5% Al_2O_3 by the same amount of MgO (YAM-1) enhances the reaction rate remarkably. While at short dwell times between 0.5 and 2 h the conversion is lower than for the 3% magnesia containing specimens (YM-2 and YM-3), the same amount of conversion is achieved after 4 h.

3.3. Effect of sample size

To reveal the influence of the specimen size on the Si conversion, different sample geometries, as shown in Fig. 1, were investigated. For the nitridation of the silicon powder the nitrogen transport into the compact might become a limiting factor for parts with larger wall thickness and/or smaller pore channels. Therefore it was expected that – if at all – *decreasing* sample size would be beneficial for the reaction rate of Si_3N_4 formation. In Fig. 4(a)–(c) the Si conversion is plotted for different dwell times in dependence of sample mass (after debinding); as each set of specimens was moulded from the same feedstock the mass can be taken also as a measure for the sample size/volume. To evaluate the role of different sintering aids the investigations included samples from the following feedstocks: YA-3, YM-3, and YAM-1.

Contrary to our expectations, as a general tendency it can be identified that with *increasing* sample mass (or volume) the Si conversion increases, independent of dwell time. For YA-3 samples shown in Fig. 4(a) only a very moderate increase of Si

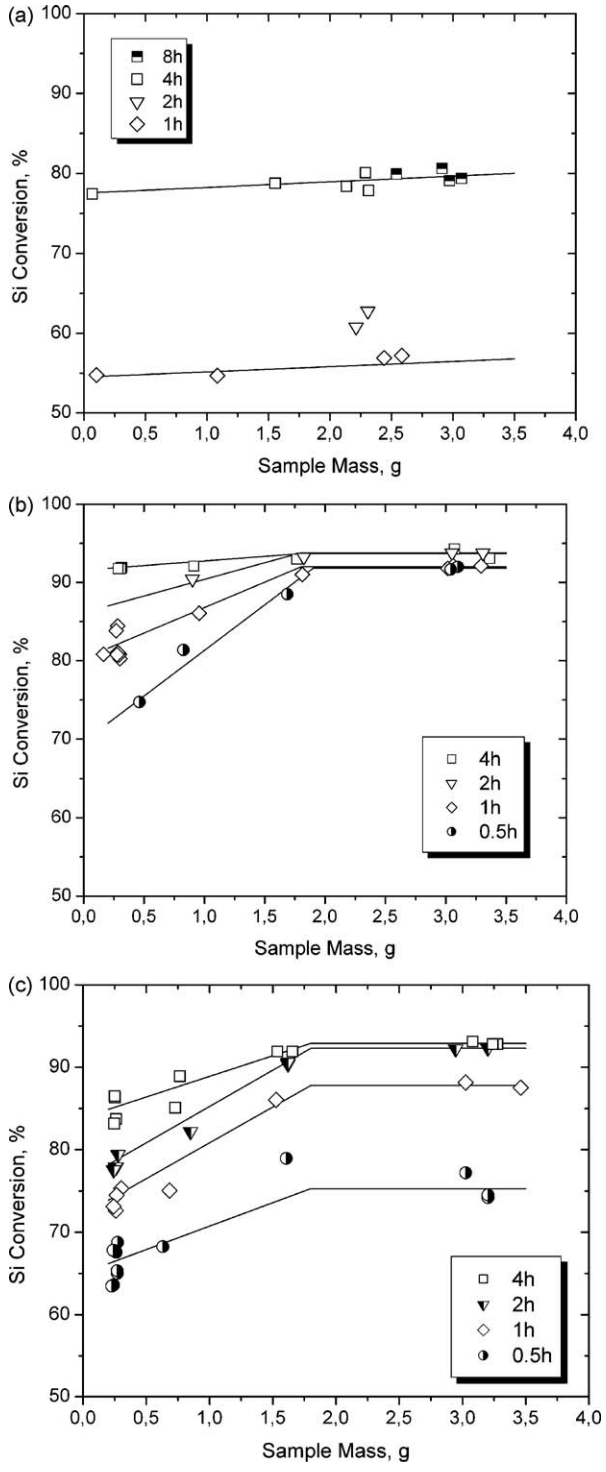

Fig. 4. Si conversion in dependence of sample mass for different dwell times at 1390 °C: (a) YA-3, (b) YM-3, and (c) YAM-1.

conversion is observed and dwell time has a much more pronounced effect on the Si_3N_4 formation. MgO containing samples of YM-3, which are presented in Fig. 4(b), exhibit not only higher Si conversion values, but also a clear relationship between sample mass and Si conversion. Especially at short dwell times (0.5 and 1 h) when the reaction is not yet completed, the size dependence is obvious. After 4 h also the small samples have reached nearly the same amount of Si conversion as the large ones and the size dependence vanishes. The conversion increases more or less linearly with sample mass up to about 1.8 g; at higher sample masses no significant further increase could be observed and a plateau is reached.

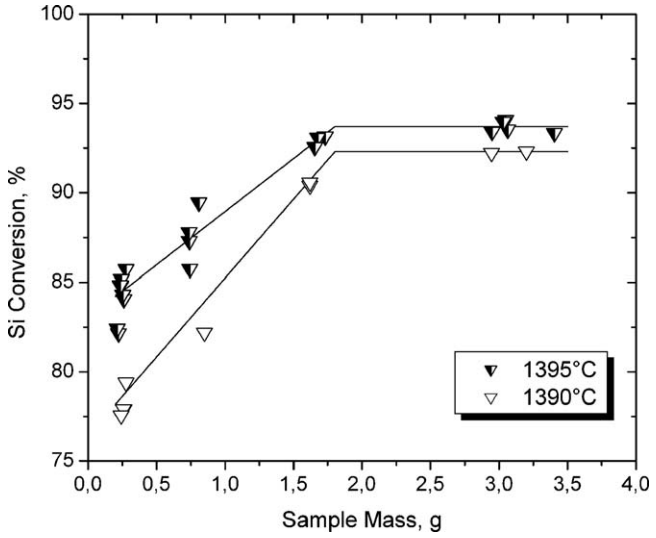

Fig. 5. Si conversion in dependence of sample mass; nitridation at 1390 °C and 1395 °C, 2 h dwell time, feedstock YAM-1.

Also for the combination of Al_2O_3 and MgO (YAM-1) a positive correlation of sample mass and Si conversion was detected (Fig. 4(c)). Similar to the YM-3 samples between 1.5 and 2.0 g the mass dependency changes from linear increase into a plateau. In contrast to YM-3, the plateau is not generally located above 90% Si conversion, but depends clearly on dwell time. After 0.5 h only 75% conversion is measured even for the largest samples.

3.4. Effect of nitridation temperature

Since silicon melts at about 1410 °C the nitridation temperature for standard processing was kept at 1390 °C as a trade-off between high reaction rate and the risk of sample deformation due to silicon melt formation. To estimate the temperature influence on Si_3N_4 formation additional nitridation experiments were conducted at 1395 °C. In Fig. 5 the Si conversion in dependence of sample mass is exemplarily plotted for YAM-1 specimens, for both temperatures after dwell time of 2 h. As expected, at 1395 °C the amount of conversion is higher than at 1390 °C; remarkably this is also true for the ‘‘plateau’’ region. When comparing the Si conversion of samples with a mass higher than 1.8 g (see Table 2), it can be concluded that increasing the temperature by just 5° is more effective than extending the dwell time from 2 to 4 h.

4. Discussion

For all powder blends – independent of amount and type of applied sintering aid, dwell time, and nitridation temperature – Si conversion never exceeded 94%. However, the gap of 6%

Table 2
Influence of dwell time and temperature on Si conversion of YAM-1.

Nitridation parameter	1390 °C/2 h	1390 °C/4 h	1395 °C/2 h
Si conversion	92.3 ± 0.2	92.9 ± 0.2	93.7 ± 0.3

weight gain does not arise from unreacted elemental Si, as revealed by XRD-analysis (Fig. 1). For the calculation of Si conversion some simplifications have been made. The weight after debinding has been taken as reference to compare samples made from feedstocks with varying binder content. It was assumed, that – beside Si – Y_2O_3, Al_2O_3, and MgO are the only constituents of the samples; residual binder as well as the inevitable SiO_2 fraction were neglected for the calculation of Si conversion. The thermal debinding step in air was limited to a temperature of 500 °C; on the one hand to keep a small amount of residual carbon binder endowing the debinded specimens with sufficient mechanical stability, and on the other hand to avoid immoderate oxidation of the silicon powder. Due to the particle size reduction by ball milling the initial oxygen content of Si certainly has been increased to more than the 0.7% specified by the supplier. Both carbon and SiO_2 can amount together to several wt.% of the sample weight, but do not contribute to a mass increase during nitridation. On the contrary, SiO_2 even may lead to a weight loss as it forms silicon monoxide above 1300 °C which is gaseous at these temperatures, following Eq. (1):

$$Si(s) + SiO_2(s) \rightarrow 2SiO(g) \quad (1)$$

Additionally, SiO_2 is able to form in combination with Y_2O_3 and N_2 crystalline secondary phases like $Y_5Si_3O_{12}N$ which were detected by X-ray analysis; although their formation causes no weight loss, less Si_3N_4 will be formed. Furthermore, the residual binder carbon of about 1% may form SiC and the equivalent amount of Si is also not available for nitrogen uptake.

The exact calculation of the Si percentage which is converted into Si_3N_4 is quite difficult to determine due to the above mentioned reasons. To find out the principal influences of different processing parameters on the nitridation of Si powder blends however, it should not be mandatory.

4.1. Influence of sample size on nitridation rate

To understand the observed correlations between sample size and Si conversion it has to be envisioned that the reaction between silicon and nitrogen Eq. (2) is exothermal [21] and that the reaction rate always increases with temperature:

$$3Si(s) + 2N_2(g) \rightarrow Si_3N_4(s)$$
$$\Delta G\,(\mathrm{kJ/mol}) = -723 + 0.315T(\mathrm{K})$$

Larger samples exhibit a smaller surface-to-volume ratio and the generated heat cannot be dissipated as fast as for smaller samples with a relatively higher surface area. Due to a higher local temperature a higher reaction rate is observed with increasing sample mass and volume. The significance of a temperature increase for the reaction rate can be observed directly when comparing the different Si conversion at 1390 and 1395 °C (Fig. 5).

On the other hand only a weak increase of Si conversion with sample mass was found for the alumina blended feedstock YA-3 (Fig. 4(a)). This observation can be explained by the generally lower reaction rate of feedstocks YA-1–YA-4 where less heat is released within a certain period of time, and heat transfer from the sample surface into the environment is effective enough so that the self-accelerating effect vanishes.

4.2. Influence of sintering aids on nitridation

A lowest melting temperature of 1282 °C has been evaluated for the Y–Si–Al–O–N system [34], and ~1200 °C is reported for the system Y–Si–Mg–O [35]. Therefore it can be expected that a liquid phase will occur during the nitridation step. However, the crystalline secondary phases which were identified in the nitrided samples are formed at relatively low temperatures of 1280 °C [12]. As these phases are stable far beyond the temperature of reaction-bonding (melting point of YN-apatite ($Y_5Si_3O_{12}N$) is 1700–1800 °C [36]), they will act as SiO_2 drain and will limit the available volume of liquid phase.

The total amount of SiO_2 is defined by the grain size of the Si powder after milling. With decreasing grain size more SiO_2 will contribute to the formation of a liquid phase during nitridation. A higher volume of liquid phase may cause blocking of the pore channels before the interior of the Si body has been completely converted [13]. The liquid phase also gives rise to a densification by shrinkage, whereby the accessible pore volume is further reduced and the reaction rate of nitridation decreases. By increasing the Y_2O_3 content Si_3N_4 formation is supported twofold: (i) the native silica covering the Si particles is removed [10] which is a prerequisite for direct reaction between silicon and nitrogen [37] and (ii) the total amount of liquid phase is reduced (and thereby premature densification) by the formation of silica-rich crystalline secondary phases.

The interaction of yttria amount and Si grain size explains quite well the experimental observations that for powder blends with equal type and amount of sintering aids but different grain size (YA-1/YA-2, YA-3/YA-4 and YAM-1/YAM-2), the finer powders exhibit slower reaction rates; and when grain size is comparable an increase of yttria content corresponds to higher reaction rates (YA-1/YA-3 and YA-2/YA-4).

Beyond these reasonable correlations, an explanation for the contrary effects of Al_2O_3 and MgO additions on the silicon nitridation has to be given. Confirming the investigations of Lee and Kim [28], it was observed that MgO allows higher nitridation rates than Al_2O_3. But by variation of the sintering aid concentrations, it was found in the present work that an *increase* of the Al_2O_3 content leads to a *decrease* of the nitridation rate, while for MgO the reaction rate increases with increasing content. From this it follows that Al_2O_3 has a retarding effect on the nitridation of silicon, at least in combination with Y_2O_3.

The reason for this opposed effects might be found in different viscosities of the liquid phase depending on different

additives. Sintering aid combinations containing MgO exhibit lower melting temperatures as well as a lower viscosity of the liquid phase than those with Al_2O_3 [35]. Although the presence of a liquid phase is in conflict to fast nitridation rates [13], it can be expected that lower liquid phase viscosity facilitates nitrogen transport to the sites of unreacted Si in comparison to a higher viscous phase. Provided that two Si/RBSN samples contain the same volume fraction of liquid phase, a lower viscosity then would correspond to higher reaction rates due to enhanced nitrogen diffusion.

5. Conclusion and outlook

The processing of SRBSN splits up into two main steps: the reaction-bonding step where a silicon powder compact is transferred into Si_3N_4 by reaction with nitrogen, and the sintering step where densification of the porous RBSN body takes place. In the present work explicitly the reaction-bonding step was examined. The boundary conditions which determined the process parameters were the shaping technology (injection moulding) and the projected application (micro-components).

With regard to the qualification as material for micro-mechanical components the unexpected observation was made, that smaller samples of few 100 mg exhibited slower reaction rates and consequently required somewhat more extended nitridation treatment than samples of a few grams. Nonetheless by choosing appropriate process parameters and sintering aids, processing times could be realized which are significantly lower than the 20–100 h dwell time reported for large scale SRBSN components.

It was confirmed that the role of the metal oxide additions is not restricted to facilitating a liquid phase for sinter-densification and that they do not behave as inert materials during the nitridation reaction. A strong influence of the type and amount of sintering aid on the reaction rate of silicon nitride formation was detected instead. For example, for MgO containing powder blends even after 0.5–1.0 h dwell time a virtually complete conversion of the available Si was achieved. While high Y_2O_3 additions also contribute to fast reaction rates, Al_2O_3 appears to act rather as an inhibitor for Si_3N_4 formation under the investigated conditions.

The primarily task of the sintering aids however, is to allow for pressureless sintering of the reaction-bonded silicon nitride. It has to be clarified in following investigations how the microstructure of the RBSN material already formed under the influence of different sintering aids behaves during densification at higher temperatures. Therefore a subsequent paper will cover the shrinkage behaviour and the shape retention along the processing route ranging from moulded to sintered components. On the basis of micro-bending tests the mechanical properties of SRBSN micro-specimen will be shown and the process/microstructure/property relations are discussed. Low-pressure injection moulded components for a micro-planetary gear and a micro-turbine will finally illustrate the general capabilities of the developed process.

Acknowledgements

The financial support provided by the German Research Foundation (DFG) in the framework of the SFB 499 is greatly appreciated. We want to thank A.C. Ferrari Felippi, Universidade Federal de Sao Carlos, Brazil, and Dr. E. Goloubtsova, Belarusian State Polytechnic Academy, Minsk, Belarus, for their support during materials processing.

References

[1] G. Ziegler, J. Heinrich, G. Wötting, Review: relationships between processing, microstructure and properties of dense and reaction-bonded silicon nitride, J. Mater. Sci. 22 (1987) 3041–3086.
[2] F.L. Riley, Silicon nitride and related materials, J. Am. Ceram. Soc. 83 (2) (2000) 245–265.
[3] G. Petzow, M. Herrmann, Silicon Nitride Ceramics, Structure and Bonding, vol. 102, Springer Verlag, Berlin/Heidelberg, 2002, pp. 47–167.
[4] S. Hampshire, Nitride ceramics, in: R.W. Cahn, P. Haasen, E.J. Kramer (Eds.), Material Science and Technology, Structure and Properties of Ceramics, vol. 11, VCH Verlagsgesellschaft, Weinheim, 1994, pp. 119–171.
[5] A. Giachello, P. Popper, Post-sintering of reaction-bonded silicon nitride, Ceram. Int. 5 (3) (1979) 110–114.
[6] P. Greil, Near net shape manufacturing of ceramics, Mater. Chem. Phys. 61 (1999) 64–68.
[7] N. Kondo, H. Hyuga, H. Kita, T. Kaba, Fabrication of thick silicon nitride by reaction bonding and post-sintering, J. Ceram. Soc. Jpn. 115 (2007) 285–289.
[8] J.R.G. Evans, A.J. Moulson, The effect of impurities on the densification of reaction-bonded silicon nitride (RBSN), J. Mater. Sci. 18 (1983) 3721–3728.
[9] X. Zhu, Y. Zhou, K. Hirao, Post-densification behaviour of reaction-bonded silicon nitride (RBSN), J. Mater. Sci. 39 (2004) 5785–5797.
[10] X. Zhu, Y. Zhou, K. Hirao, Processing and thermal conductivity of sintered reaction-bonded silicon nitride I: effect of Si powder characteristics, J. Am. Ceram. Soc. 89 (2006) 3331–3339.
[11] S.Y. Lee, K. Amoako-Appiagyei, H.D. Kim, Effect of β-Si_3N_4 seed crystal on the microstructure and the mechanical properties of sintered reaction-bonded silicon nitride, J. Mater. Res. 14 (1999) 178–184.
[12] H.J. Kleebe, G. Ziegler, Influence of crystalline secondary phases on the densification behaviour of reaction-bonded silicon nitride during post-sintering under increased nitrogen pressure, J. Am. Ceram. Soc. 72 (12) (1989) 2314–2317.
[13] J.S. Lee, J.H. Mun, B.D. Han, H.D. Kim, B.C. Shin, I.S. Kim, Effect of raw-Si particle size on the properties of sintered reaction-bonded silicon nitride, Ceram. Int. 30 (2004) 965–976.
[14] J.A. Mangels, Development of injection molded reaction bonded Si_3N_4, in: J.J. Burke, E.N. Lenoe, R.N. Katz (Eds.), Ceramics for High Performance Applications, vol. II, Brook Hill Publishing Co., Chestnut Hill, MA, USA, 1978, pp. 113–130.
[15] S.J. Kwak, E. Krug, S.C. Danforth, Fracture strength of low-pressure injection moulded reaction-bonded silicon nitride, J. Mater. Sci. 26 (1991) 3809–3812.
[16] G. Wötting, L. Frassek, G. Leimer, L. Schönfelder, Application-oriented development of high-performance-Si_3N_4 material and components, cfi/Ber. DKG 70 (1993) 287–294.
[17] T. Kosmac, R. Janssen, Low-pressure injection moulding of SiC platelet reinforced reaction bonded silicon nitride, J. Mater. Sci. 32 (1997) 469–474.
[18] H. Baltes, O. Brand, G.K. Fedder, C. Hierold, J.G. Korvink, O. Tabata, Advanced micro and nanosystems, in: D. Löhe, J. Haußelt (Eds.), Microengineering in Metals and Ceramics, vols. 3–4, Wiley-VCH, Weinheim, 2005.
[19] B. Kasanická, M. Müller, M. Auhorn, V. Schulze, W. Bauer, T. Beck, H.J. Ritzhaupt-Kleissl, D. Löhe, Correlations between production process,

states and mechanical properties of microspecimens made of zirconia, Microsyst. Technol. 12 (2006) 1133–1141.
[20] M. Müller, J. Rögner, B. Okolo, W. Bauer, H.J. Ritzhaupt-Kleissl, Factors influencing the mechanical properties of moulded zirconia micro parts, in: J.G. Heinrich, C. Aneziris (Eds.), Proc. 10th ECerS Conf., Göller Verlag, Baden-Baden, 2007, pp. 1291–1296.
[21] A.J. Moulson, Review: reaction-bonded silicon nitride—its formation and properties, J. Mater. Sci. 14 (1979) 1017–1051.
[22] H.M. Jennings, On reactions between silicon and nitrogen, J. Mater. Sci. 18 (1983) 951–967.
[23] R.G. Pigeon, A. Varma, Some factors influencing the formation of reaction-bonded silicon nitride, J. Mater. Sci. 28 (1993) 1919–1936.
[24] R.G. Pigeon, A. Varma, Quantitative kinetic analysis of silicon nitridation, J. Mater. Sci. 28 (1993) 2999–3013.
[25] Z.R. Jovanovic, Kinetics of direct nitridation of pelletized silicon grains in a fluidized bed: experiment, mechanism, modelling, J. Mater. Sci. 33 (1998) 2339–2355.
[26] V. Pavarajarn, S. Kimura, Catalytic effects of metals on direct nitridation of silicon, J. Am. Ceram. Soc. 84 (2001) 1669–1674.
[27] H. Hyuga, K. Yoshida, N. Kondo, H. Kita, J. Sugai, H. Okano, J. Tsuchida, Nitridation enhancing effect of ZrO_2 on silicon powder, Mater. Lett. 62 (2008) 3475–3477.
[28] B.T. Lee, H.D. Kim, Effect of sintering additives on the nitridation behaviour of reaction-bonded silicon nitride, Mater. Sci. Eng. A 364 (2004) 126–131.
[29] Y. Zhang, Effects of additives on the nitridation process of foamed materials containing silicon and silicon carbide powders, Mater. Res. Bull. 39 (2004) 401–407.
[30] W. Bauer, R. Knitter, Development of a rapid prototyping process chain for the production of ceramic microcomponents, J. Mater. Sci. 37 (2002) 3127–3140.
[31] S. Kolitsch, H.J. Seifert, T. Ludwig, F. Aldinger, Phase equilibria and crystal chemistry in the Y_2O_3–Al_2O_3–SiO_2 system, J. Mater. Res. 14 (1999) 447–455.
[32] F.M. Mahoney, Sinterverhalten und Phasenbeziehungen von Si_3N_4-Keramiken im System Si_3N_4–SiO_2–MgO–Y_2O_3, Ph.D. Thesis, University of Stuttgart, Germany, 1992.
[33] M.K. Kim, J.K. Park, H.W. Lee, S. Kang, A cyclic process for the nitridation of Si powder, Mater. Sci. Eng. A 408 (2005) 85–91.
[34] D. Matusch, Phasenuntersuchungen im System Y–Si–Al–O–N, Ph.D. Thesis, University of Stuttgart, Germany, 2003.
[35] T.N. Tiegs, F.C. Montgomery, J.L. Schroeder, D.L. Barker, P.A. Menchhofer, Effect of powder characteristics on the alpha-to-beta Si_3N_4 transformation kinetics, Am. Ceram. Soc. 18 (4) (1997) 437–447 (Ceramic Engineering & Science Proceedings).
[36] T. Nishimura, M. Mitomo, Phase relationships in the system Si_3N_4–SiO_2–Yb_2O_3, J. Mater. Res. 10 (1995) 240–242.
[37] M.N. Rahaman, A.J. Moulson, The removal of surface silica and its effects on the nitridation of high-purity silicon, J. Mater. Sci. 19 (1984) 189–194.